Characterization of genetic and molecular tools for studying the endogenous expression of *Lactate dehydrogenase* in *Drosophila melanogaster*

Madhulika Rai[1], Sarah M. Carter[1], Shefali A. Shefali[1], Geetanjali Chawla[2]*, Jason M. Tennessen[1]*

[1]Department of Biology, Indiana University, Bloomington, IN 47405, USA
[2]Department of Life Sciences, School of Natural Sciences, Shiv Nadar Institute of Eminence, Dadri, Uttar Pradesh 201314, India

*Co-corresponding author

Email: geetanjali.chawla@snu.edu.in and jtenness@indiana.edu

Key words: *Drosophila melanogaster,* metabolism, Lactate dehydrogenase

ABSTRACT

Drosophila melanogaster larval development relies on a specialized metabolic state that utilizes carbohydrates and other dietary nutrients to promote rapid growth. One unique feature of the larval metabolic program is that Lactate Dehydrogenase (Ldh) activity is highly elevated during this growth phase when compared to other stages of the fly life cycle, indicating that Ldh serves a key role in promoting juvenile development. Previous studies of larval Ldh activity have largely focused on the function of this enzyme at the whole animal level, however, *Ldh* expression varies significantly among larval tissues, raising the question of how this enzyme promotes tissue-specific growth programs. Here we characterize two transgene reporters and an antibody that can be used to study *Ldh* expression *in vivo*. We find that all three produce similar *Ldh* expression patterns. Moreover, these reagents demonstrate that the larval *Ldh* expression pattern is complex, suggesting the purpose of this enzyme varies across cell types. Overall, our studies validate a series of genetic and molecular reagents that can be used to study glycolytic metabolism in the fly.

INTRODUCTION

Lactate dehydrogenase (Ldh) is a highly conserved enzyme that serves a key role in the regulation of cellular redox balance, glycolytic metabolism, and energy production [1, 2]. Although this enzyme has been studied for over a century [3] [4], we are still discovering new functions for Ldh in metabolism, signal transduction, and even gene expression [1, 2, 5-8]. Moreover, due to the central role that Ldh serves in cellular physiology, a wide variety of human diseases are associated with changes in Ldh expression and activity. For example, Ldh is well-known to play a central role in tumor metabolism, and enhanced Ldh serum levels are used as one of the diagnostic parameters in oral, laryngeal, melanoma, renal cell carcinoma and breast cancers, [9-12]. The role of Ldh in human disease, however, extends far beyond cancer metabolism, as enhanced Ldh activity is also observed in diabetes and hyperglycemia [13-16], as well as during viral infections [17, 18]. In this regard, despite the well-documented relationship between elevated Ldh activity and human disease progression, questions remain about the tissue-specific mechanisms that link changes in Ldh expression and activity with the overall disruption of human health.

The fruit fly *Drosophila melanogaster* has emerged as an ideal system to study the role of Ldh in both healthy and diseased tissues. For example, Ldh activity levels fluctuate during the life-cycle in a predictable manner [19, 20]. In this regard, Ldh clearly plays a significant role during larval development, when the animal experiences a nearly 200-fold increase in body mass [21]. Ldh expression and activity are very high during this growth phase when compared to other phases of fly life-cycle [19], indicating that lactate production is important for larval metabolism. Consistent with this hypothesis, *Ldh*

mutations render larvae unable to maintain a normal redox balance, and when combined with *Gpdh1* mutations, induce significant growth defects [22]. In this manner, studies of Ldh provide an opportunity to understand how changes in Ldh expression affect *Drosophila* growth, development, and life-history events.

Similarly, studies of *Drosophila* disease models have also begun to focus on the link between lactate metabolism activity and tumor growth [for review, see 23], neuronal health and aging [24-27], as well as during infections and immune challenges [28]. Notable among these findings is that *Drosophila* tumors up-regulate Ldh in a manner that mimics the elevated Ldh-A activity observed in many human cancer cells [23, 29-33], indicating that Ldh in both flies and humans serves a beneficial role in tumorous growth. Thus, studies of *Drosophila* Ldh hold the potential to better understand how mammalian Ldh homologs function in development and disease.

Several genetic and molecular reagents have been used to examine *Drosophila* Ldh expression and activity. For example, early studies of Ldh in the fly relied on a biochemical enzymatic assay that generated an easily visualized staining pattern [30, 34]. These enzymatic assays have been supplemented with transgenes that rely on fluorescent proteins to either directly or indirectly visualize *Ldh* gene expression[28, 30, 32, 35]. However, most published *Ldh* reporters have not been directly compared, either with each other or with endogenous protein expression, raising the possibility that published genetic reagents might produce artifactual results. To address this issue and thus facilitate more precise studies of *Drosophila* Ldh function, here we compare the following genetic and molecular reagents: (i) a previously described *Ldh* genomic rescue construct that consists of a green fluorescent protein (GFP) coding region

inserted immediately before the *Ldh* stop codon (referred to as *Ldh-GFP*^{Genomic}**)** [32], (ii) a previously described *Ldh-GFP* reporter that consists of *EGFP* inserted 50 bp upstream of the endogenous start site (referred to as *Ldh-GFP*^{enhancer}) [36] [30], and (iii) a commercially available *Drosophila* Ldh antibody (see methods). As described below, we demonstrate that *Ldh-GFP*^{Genomic} produces a functional enzyme capable of rescuing the *Ldh* mutant phenotypes. Moreover, our studies reveal that all three reagents generate similar tissue-specific *Ldh* expression patterns. Interestingly, our analyses also reveal that Ldh is expressed in a complex manner during larval development, suggesting that this enzyme functions in multiple cell- and tissue-specific roles during larval development. Overall, our study enhances the ability of the *Drosophila* community to study Ldh within the context of both normal developmental as well as human disease models.

METHODS

Drosophila melanogaster husbandry and genetic analysis

Fly stocks were maintained at 25ºC on Bloomington Drosophila Stock Center (BDSC) food. Larvae were raised and collected as previously described [37]. Briefly, 50 adult virgin females and 25 males were placed into a mating bottle and embryos were collected for 4 hrs on a 35 mm molasses agar plate with a smear of yeast paste on the surface. Collected plates were stored inside an empty 60 mm plastic plate and placed in a 25ºC incubator.

Ldh mutations were maintained in trans to the balancer chromosome *TM3, p{Dfd-GMR-nvYFP}, Sb*^{1} (BDSC Stock 23231). Unless noted, *Ldh* mutant larvae harbored a trans-heterozygous combination of *Ldh*^{16} and *Ldh*^{17} as described in previous studies [38].

Two transgenes were examined in our study. The *p{Ldh-GFP}* transgene was generated by inserting GFP immediately upstream of the *Ldh* stop codon within a previously described *Ldh* genomic rescue construct [32, 38]. For our analysis, the *p{Ldh-GFP}* was placed in the background of *Ldh* loss-of-function allele *Ldh*^{16} [38]. The previously described *Ldh-GFP* enhancer trap line was a kind gift from Utpal Banerjee's lab [30, 36]. Finally, the *p{Ldh-mCherry}* transgene, which was previously described in a study of *Drosophila* hemocyte metabolism [28], is identical to the *p{Ldh-GFP}* except that the *mCherry* coding sequence was inserted immediately upstream of the *Ldh* stop codon. To distinguish between the two *Ldh-GFP* and the *Ldh-mCherry* constructs in the text, we will refer to the *p{Ldh-GFP}* and *p{Ldh-mCherry}* rescuing transgenes as *Ldh-GFP*^{Genomic} and *Ldh-mCherry*^{Genomic}, respectively, and the *Ldh-GFP*

enhancer trap line will be referred to as *Ldh-GFP*^{Enhancer}.

Viability assay

Larval viability was measured by placing 20 synchronized embryos of each genotype on molasses agar plates with yeast paste and measuring time until pupariation. Wandering L3 larvae were subsequently transferred into a glass vial containing BDSC food and monitored until eclosion.

Immunofluorescence Assay

Larval tissues were dissected from mid-third instar larvae in 1X phosphate buffer saline (PBS; pH 7.0) and fixed with 4% paraformaldehyde in 1X PBS for 30 minutes at room temperature. Fixed samples were subsequently washed once with 1X PBS and twice with 0.3% PBT (1x PBS with Triton X-100) for 10 mins per wash.

For antibody staining of GFP in larvae expressing either *Ldh-GFP* ^{genomic} or *Ldh-GFP*^{Enhancer}, tissues were dissected, fixed and incubated with goat serum blocking buffer (4% Goat Serum, 0.3% PBT) for one hour at RT and stained overnight at 4ºC with the primary antibody rabbit anti-GFP diluted 1:500 (#A11122 Thermo Fisher). Samples were washed three times using 0.3% PBT and stained with secondary antibody Alexa Fluor 488 Goat anti-Rabbit diluted 1:1000 (#R37116; Thermo Fisher) for either 4 hrs at room temperature or overnight at 4ºC. Stained tissues were washed with 0.3% PBT, immersed in DAPI (0.5µg/ml 1X PBS) for 30 mins and then mounted with vector shield with DAPI (Vector Laboratories; H-1200-10).

For larval tissues stained with the anti-Ldh antibody (Bosterbio; DZ41222), fixed

tissues were washed three times with 0.03% PBT for 10 minutes and incubated in blocking buffer (3% bovine serum albumin) for 15 mins on a rocking shaker at room temperature. Tissues were then incubated with 200 μl of blocking buffer containing a 1:20 dilution of anti-Ldh on a rocking shaker for 12 hrs at room temperature, 12 hrs at 4ºC, and a third incubation of 12 hrs at room temperature. Samples were then washed twice using 200 μl of blocking buffer with a 10 min room temperature incubation for each wash. Once the second wash was removed, 200 μl of blocking buffer containing a 1:1000 dilution of goat anti-rabbit Alexa 488 (Thermo Fisher; catalog #R37116) was added to the well and samples were incubated overnight on a rocking incubator at 4 ºC. The next day, tissues were washed twice with blocking buffer, once with 0.03% PBT, once with PBS, and subsequently incubated for 15 mins in PBS containing 0.5 µg/ml of DAPI. Stained tissues were then mounted using vector shield containing DAPI (Vector Laboratories; H-1200-10).

For all imaging studies, multiple Z-stacks of individual tissues were acquired using the Leica SP8 confocal microscope in the Light Microscopy Imaging Center at Indiana University, Bloomington.

Gas Chromatography-Mass Spectrometry (GC-MS) analysis

Samples were collected, processed, and analyzed as previously described [39, 40]. For all experiments, six biological replicates containing 25 mid-L2 larvae were analyzed per genotype. GC-MS data was normalized based on sample mass and internal succinic-d4 acid standard.

Statistical analysis of metabolite data

Statistical analysis was conducted using GraphPad Prism v9.1. Metabolic data are presented as scatter plots, with the error bars representing the standard deviation and the line in the middle representing the mean value. Data were compared using a Kruskal–Walli's test followed by a Dunn's multiple comparison test.

RESULTS

Genetic characterization of the *Ldh-GFP*^{Genomic} transgene

As a first step towards validating reagents for studying Ldh expression, we initially examined a GFP-tagged genomic rescue construct, referred to here as *Ldh-GFP*^{Genomic}, which has been previously used to study muscle development and imaginal discs tumors [32]. As described above and elsewhere, this transgene consists of a fragment of genomic DNA that contains the entire *Ldh* locus with GFP inserted at the 3' end of the coding sequence, immediately prior to the stop codon. To determine if the *Ldh-GFP*^{Genomic} generates a functional GFP-tagged fusion protein, we assayed the ability of this transgene to rescue *Ldh* mutant phenotypes. Our genetic approach revealed that the resulting fusion protein appears functional, as the *Ldh-GFP*^{Genomic} transgene rescues both the lethal phenotype and metabolic defects displayed by *Ldh*$^{16/17}$ mutant larvae (Figure 1C-E) [38]. We would note, however, that *Ldh-GFP*^{Genomic}*; Ldh*$^{16/17}$ mutant larvae exhibited slightly decreased levels of lactate and 2-hydroxyglutarate (2HG) as compared with the wild-type control (Figure 1D,E), suggesting the resulting fusion protein harbors lower activity than the endogenous enzyme. Overall, these results indicate that *Ldh-GFP*^{Genomic} produces a functional Ldh enzyme.

In addition to assessing Ldh-GFP enzymatic function, we also assayed the gross expression pattern of *Ldh-GFP*^{Genomic}. Previous studies have demonstrated that Ldh is highly active during larval development relative to other developmental stages – peaking during the L3 stage and gradually declining during the wandering stage and early metamorphosis [19]. Consistent with previous observations, we noted that *Ldh-GFP*^{Genomic} is expressed at such a high level during larval development that GFP was

apparent in live larvae using a standard dissecting microscope. Overall, these whole animal expression levels mimicked previously reported changes in larval Ldh enzyme expression and activity, with Ldh-GFP levels peaking in the L3 stage and declining thereafter. We would also note that *Ldh-GFP*^{Genomic} is so highly expressed in the larval central nervous system (CNS) and body wall muscles that GFP fluorescence from these tissues can easily be observed under low magnifications (Figure 1E). Overall, the observed *Ldh-GFP*^{Genomic} expression pattern is consistent with previous biochemical and genetic studies, as well as a recent manuscript that used this transgene to examine Ldh expression within body wall muscle [32]

In addition to the *Ldh-GFP*^{Genomic} transgene, we have also generated an identical version of this transgene labeled with mCherry, referred to herein as *Ldh-mCherry*^{Genomic}, which was previously used to study hemocyte metabolism [28]. In general, the *Ldh-GFP*^{Genomic} and *Ldh-mCherry*^{Genomic} transgenes exhibit similar spatial expression patterns, with notably high expression in the CNS and muscle (Figure S1). However, the Ldh-mCherry fusion protein persists throughout much of metamorphosis (compare Figure 1E with S1C), suggesting that this fusion protein is either stabilized or accumulates to a higher level than Ldh-GFP. Since the *Ldh-GFP*^{Genomic} expression pattern more accurately reflects previously reported temporal changes in Ldh expression and activity, we chose to only characterize *Ldh-GFP*^{Genomic} in our subsequent experiments.

Ldh is expressed in a complex pattern during larval development

Our analysis of the *Ldh-GFP*^{Genomic} transgene indicates that this genetic reagent can

be used to reliably analyze *Ldh* expression. To further assess this possibility, we compared the tissue-specific larval expression pattern of the *Ldh-GFP*^{Genomic} transgene with *Ldh-GFP*^{enhancer}, as well as a previously undescribed *Drosophila* Ldh antibody (see methods; note that αLdh does not stain *Ldh*$^{16/17}$ mutant tissues; Figure S2). Our comparison demonstrated that all three reagents produced a similar cell- and tissue-specific larval staining pattern. Below we provide a brief description of the *Ldh* expression pattern in L3 larvae raised under standard growth conditions.

Central Nervous System: The complexity of the *Ldh* expression pattern is perhaps most apparent in the central nervous system, where *Ldh* was highly expressed in the central brain and ventral nerve chord but absent from the optic lobe region (medulla, neuroepithelia and lamina; Figure 2A-L). At the level of individual cell types, we observed *Ldh* expression in a subset of ganglion mother cells (GMCs, Figure 3E-H), neurons (Figure 3I-L) and glia (Figure 3M-P), but not in neuroblasts (Figure 3A-D). We are unsure as to why Ldh is only present within a subset of GMCs, neurons, and glia.

Digestive and Renal Systems: Both the larval gut and Malpighian tubules express Ldh in cell-specific manner. Within the gut, *Ldh* was expressed at relatively high levels in subset of cells within the AMP clusters but at low or undetectable levels within larger EC cells (Figure 4A-F). We are uncertain as to why only a subset of these cells express such high Ldh levels. In the Malpighian tubules, high Ldh levels were observed only in stellate cells (Figure 4G-L).

Fat Body and Salivary Glands: Previous studies of the Ldh enzyme activity suggest that Ldh expression levels are relatively low in the larval salivary glands and fat body. Consistent with this observation, Ldh expression was below the level of detection within both the fat body (Figure 5A-F) and salivary glands (Figure 5G-L).

Imaginal discs: Ldh expression has been extensively studied in the larval imaginal discs [23, 29-33]. These studies have consistently observed relatively low levels of *Ldh* expression during normal imaginal disc development. Our findings confirm earlier studies and again demonstrate that *Ldh* is present at a relatively low level within the leg, wing, and eye-antennal imaginal discs from L3 larvae (Figure 6A-L). However, we found that *Ldh* is noticeably expressed within a few cells of these tissues. Patches of GFP expression were observed in the leg disc, which based on the similarity of this expression with that of *sens* [41] [42], we hypothesize to be the sensory organ precursors (SOPs). Also, both transgenic constructs resulted in GFP expression in cells of the eye-antennal disc posterior to the morphogenetic furrow (Figure 6E,F,K,L).

Overall, the similarities in expression between the *Ldh-GFP*^{Genomic} transgene, the *Ldh-GFP*^{enhancer} transgene, and the αLdh antibody in the examined larval tissues suggests that the *Drosophila* metabolism community can use any of these three reagents to study Ldh. However, we would recommend that any future study uses more than one of these reagents to validate observed changes in Ldh expression.

DISCUSSION

Here we demonstrate that two transgenes and a commercially available antibody reveal similar *Ldh* expression signatures during larval development. While the *Ldh-GFP*^{Genomic} and *Ldh-GFP*^{enhancer} transgenes were previously described and used for a variety of studies, our analysis indicates that either reagent can be used to reliably study *Ldh* expression. Moreover, our characterization of the *Ldh* antibody provides the first direct visualization of Ldh protein within the fly and will significantly enhance future studies of this enzyme. Overall, our study thus validates use of these reagents for future use by the *Drosophila* research community.

Beyond our initial validation of these three reagents, our study also reveals that *Ldh* is expressed in a complex pattern across tissues and cell-types. At the gross tissue level, our analysis agrees with studies dating back to the 1970s [19], as well as modern gene expression analyses that described how *Ldh* expression varies in intensity across larval tissues [28, 30, 32, 35, 43]. Consistent with those early studies, we observe very high Ldh expression in muscle and relatively low or undetectable levels in the fat body and salivary glands. All three observations are interesting in regard to the metabolism of those tissues. For example, while high levels of *Ldh* expression in larval muscle would be expected based on the role of this enzyme in a wide variety of other animals, adults exhibit relatively low levels of *Ldh* activity [19], indicating that *Drosophila* muscle has evolved to meet the extreme energetic demands without using this enzyme and raising the question as to why there is such a dramatic difference in *Ldh* expression levels between larval and adult muscle. One likely explanation is that *Ldh* in the muscle, as well as other larval tissues, serves to buffer mitochondrial metabolism

against the hypoxic environments often encountered by Dipteran larvae – a hypothesis supported by earlier studies [44, 45]. Future studies should both examine this possibility and investigate why larval salivary glands and fat body exhibit relatively low *Ldh* activity levels.

In contrast to the muscle, fat body, and salivary glands, other larval tissues display a complex expression pattern. For examples, the AMP clusters of the larval midgut and stellate cells in the Malphigian tubules exhibit notably high levels of Ldh expression relative to other cell types in the surrounding tissue. The larval CNS, however, exhibits the most dramatic example of how Ldh expression can vary across cell types. Notably, there is a striking lack of *Ldh* expression in neuroblasts relative to other cell-types. Moreover, while we observe *Ldh* in both neurons and glia – a result consistent with the current hypothesis that lactate functions in a metabolic shuttle between these two cells types [24, 46]. However, we observed an unexpected heterogeneity in expression levels throughout the brain, with regions of high Ldh expression being observed adjacent to low levels. We are uncertain as to the significance of this observation.

Finally, we would highlight the distinct lack of *Ldh* in larval imaginal discs at the timepoint examined. Our observation is consistent with several previous studies, which describe how *Ldh* is expressed at low levels in normal imaginal discs but at dramatically higher levels in tumorous discs [23, 29-33]. Together, these suggest that the presence or absence of *Ldh* within the discs are of importance for cell growth and development. We would also note that much earlier studies supported a model in which *Ldh* expression is somehow linked to imaginal disc development. After all, the original

name for *Ldh* in *Drosophila melanogaster* was *Imaginal disc membrane protein L3* (*ImpL3*) [34, 47], which was identified as being induced in response to 20-hydroxyedcysone signaling. Consistent with this possibility, imaginal discs exposed to 20-hydroxyecdysone in culture exhibit a significant increase in *Ldh* expression [34]

In conclusion, our study validates the use of both genetic and molecular reagents to accurately study *Ldh* expression during larval development. Moving forward, we would encourage the fly community to use these reagents in combination when conducting studies of *Ldh* expression.

FIGURE LEGENDS

Figure 1. Genetic characterization of the *p{Ldh-GFP}* transgene. (A) A schematic diagram of the *Ldh-GFP*^{Genomic} transgene illustrating the placement of GFP immediately before the *Ldh* stop codon. When this transgene is placed in a *Ldh*$^{16/17}$ mutant background, the resulting Ldh-GFP fusion protein is capable of not only rescuing (B) the *Ldh* mutant lethal phenotype, but also restoring steady state levels of (C) lactate and (D) 2-hydroxyglutarate (2HG). (E) The *Ldh-GFP*^{Genomic} temporal expression pattern is consistent with previous studies, with Ldh-GFP^{Genomic} being expressed at high levels throughout larval development and then declining at the onset of metamorphosis. Data in (B-D) analyzed using one-way ANOVA followed by a post hoc Tukey HSD. ***P<0.001.

Figure 2. Characterization of *Ldh* expression in the central nervous system. The *Ldh* expression pattern in the central nervous system of L3 larvae was examined using *Ldh-GFP*^{Genomic}, *Ldh-GFP*^{enhancer}, and an αLdh antibody. (A-L) Representative confocal images of Ldh expression and DAPI staining in the (A-F) ventral and (G-L) dorsal sides of the CNS. For *Ldh-GFP*^{Genomic} and *Ldh-GFP*^{enhancer} expression analysis, the CNS was fixed and stained with an αGFP antibody as described in the methods. The scale bar in all images represents 40 μM. Scale bar in (A) applies to (B,G,H). Scale bar in (C) applies to (D,I,J). Scale bar in (E) applies to (F,K,L).

Figure 3. *Ldh* expression in ganglion mother cells, neurons, and glia. Representative confocal images showing the absence of *Ldh* in neuroblasts of third instar *Ldh-GFP* ^{genomic} larvae. The first two columns from left to right show DAPI and Ldh. The last column shows the colocalization of *Ldh* with CNS cell specific markers. (A-D) *Ldh* is not expressed in neuroblasts, which are labelled with αMiranda (MIRA) antibody. In contrast, (E-H) *Ldh* is expressed in ganglion mother cells (GMCs), which are labelled with αProspero (PROS) antibody. Ldh-GFP is also present in both (I-K) neurons stained with αElav and (M-P) and glia stained with αRepo. For *Ldh-GFP*^{Genomic} and *Ldh-GFP*^{enhancer} expression analysis, the CNS was fixed and stained with an αGFP antibody as described in the methods. The scale bar in all images represents 40 μM. Scale bar in (A) applies to B-D). Scale bar in (E) applies to (F-H). Scale bar in (I) applies to (J-L). Scale bar in (M) applies to (N-P).

Figure 4. Characterization of *Ldh* expression in the intestine and Malpighian tubules. The *Ldh* expression pattern in the intestine and Malphigian tubules of L3 larvae was examined using *Ldh-GFP*^{Genomic}, *Ldh-GFP*^{enhancer}, and an αLdh antibody. (A-L) Representative confocal images of *Ldh* expression and DAPI staining in (A-F) the midgut and (G-L) the Malphigian tubules. Note that *Ldh* is expressed at significantly higher levels in (A,C,E) a subset of small cells of the AMP clusters (denoted with arrowheads in (A-F))

and (G,I,K) the stellate cells of the Malpighian tubules. For *Ldh-GFP*^{Genomic} and *Ldh-GFP*^{enhancer} expression analysis, tissues were fixed and stained with an αGFP antibody as described in the methods. The scale bar in all images represents 40 μM.

Figure 5. *Ldh* expression pattern in the fat body and salivary gland. The *Ldh* expression patterns in the fat body and salivary glands of L3 larvae were examined using *Ldh-GFP*^{Genomic} and *Ldh-GFP*^{enhancer}. (A-L) Representative confocal images of *Ldh* expression and DAPI staining in (A-F) the fat body and (G-L) the salivary glands. For *Ldh-GFP*^{Genomic} and *Ldh-GFP*^{enhancer} expression analysis, tissues were fixed and stained with an αGFP antibody as described in the methods. The scale bar in all images represents 40 μM.

Figure 6. *Ldh* expression pattern in Imaginal discs. Representative confocal images of imaginal discs (top to bottom: wing disc, leg disc and eye disc) dissected from third instar (D5 AEL) *Ldh-GFP* ^{genomic} (A-F) and *Ldh-GFP*^{enhancer} (G-L) third instar larvae. DAPI is shown in white and *Ldh* expression is shown in green. Note that the αLdh antibody failed to produce any staining in the imaginal discs and thus was excluded from the figure. The scale bar in all images represents 40 μM.

SUPPLEMENTAL FIGURES LEGENDS

Figure S1. Expression of *Ldh-mCherry*^{Genomic} during larval development. The *Ldh-mCherry*^{Genomic} spatial expression pattern is consistent with previous studies, with Ldh-mCherry^{Genomic} being expressed at high levels in (A) the body wall muscle. However, unlike Ldh-GFP^{Genomic}, the (A) expression of mCherry^{Genomic} fusion protein persists throughout much of pupal development (compare with Figure 1B).

Figure S2. αLdh immunostaining in control and *Ldh* mutant larval tissues. Representative confocal images of the (A-H) central nervous system, (E-H) intestine, (I-L) fat body, and (M-P) salivary gland dissected from third instar w^{1118} and Ldh^{16} larvae. DAPI is shown in white and *Ldh* expression is shown in green. Note the brightness in (L) was increased to highlight the lack of staining in small cells within AMP clusters. The scale bar in all images represents 40 μM. The scale bar in (A) applies to panels (B-H), the scale bar in (I) applies to panels (J-L), and the scale bar in (M) applies to panels (N-P).

ACKNOWLEDGEMENTS

We thank the Bloomington *Drosophila* Stock Center (NIH P40OD018537) for providing fly stocks, the *Drosophila* Genomics Resource Center (NIH 2P40OD010949) for genomic reagents, Flybase (NIH 5U41HG000739), and the Indiana University Light Microscopy Imaging Center. Targeted GC-MS analysis was conducted using instruments housed in the Indiana University Mass Spectrometry Facility, which is supported, in part, by NSF MRI Award 1726633. G.C is supported by the DBT/Wellcome Trust India Alliance Fellowship/Grant [grant number IA/I(S)/17/1/503085]. J.M.T. is supported by the National Institute of General Medical Sciences of the National Institutes of Health under a R35 Maximizing Investigators' Research Award (MIRA; 1R35GM119557).

References

1. Rabinowitz JD, Enerback S. Lactate: the ugly duckling of energy metabolism. Nat Metab. 2020;2(7):566-71. Epub 20200720. doi: 10.1038/s42255-020-0243-4. PubMed PMID: 32694798; PubMed Central PMCID: PMCPMC7983055.

2. Brooks GA. The Science and Translation of Lactate Shuttle Theory. Cell Metab. 2018;27(4):757-85. doi: 10.1016/j.cmet.2018.03.008. PubMed PMID: 29617642.

3. Fletcher WM. Lactic acid in amphibian muscle. J Physiol. 1907;35(4):247-309. doi: 10.1113/jphysiol.1907.sp001194. PubMed PMID: 16992858; PubMed Central PMCID: PMCPMC1465827.

4. Meyerhof O. Über die Energieumwandlungen im Muskel. Pflüger's Archiv für die gesamte Physiologie des Menschen und der Tiere. 1920;182(1):284-317. doi: 10.1007/BF01723748.

5. Liberti MV, Locasale JW. Histone Lactylation: A New Role for Glucose Metabolism. Trends Biochem Sci. 2020;45(3):179-82. Epub 20191231. doi: 10.1016/j.tibs.2019.12.004. PubMed PMID: 31901298.

6. Zhang D, Tang Z, Huang H, Zhou G, Cui C, Weng Y, et al. Metabolic regulation of gene expression by histone lactylation. Nature. 2019;574(7779):575-80. Epub 20191023. doi: 10.1038/s41586-019-1678-1. PubMed PMID: 31645732; PubMed Central PMCID: PMCPMC6818755.

7. Ferguson BS, Rogatzki MJ, Goodwin ML, Kane DA, Rightmire Z, Gladden LB. Lactate metabolism: historical context, prior misinterpretations, and current understanding. Eur J Appl Physiol. 2018;118(4):691-728. Epub 20180110. doi: 10.1007/s00421-017-3795-6. PubMed PMID: 29322250.

8. Lagarde D, Jeanson Y, Portais JC, Galinier A, Ader I, Casteilla L, et al. Lactate Fluxes and Plasticity of Adipose Tissues: A Redox Perspective. Front Physiol. 2021;12:689747. Epub 20210630. doi: 10.3389/fphys.2021.689747. PubMed PMID: 34276410; PubMed Central PMCID: PMCPMC8278056.

9. Nagler RM, Lischinsky S, Diamond E, Klein I, Reznick AZ. New insights into salivary lactate dehydrogenase of human subjects. J Lab Clin Med. 2001;137(5):363-9. doi: 10.1067/mlc.2001.114710. PubMed PMID: 11329534.

10. Armstrong AJ, George DJ, Halabi S. Serum lactate dehydrogenase predicts for overall survival benefit in patients with metastatic renal cell carcinoma treated with inhibition of mammalian target of rapamycin. J Clin Oncol. 2012;30(27):3402-7. Epub 20120813. doi: 10.1200/JCO.2011.40.9631. PubMed PMID: 22891270.

11. Balch CM, Soong SJ, Atkins MB, Buzaid AC, Cascinelli N, Coit DG, et al. An evidence-based staging system for cutaneous melanoma. CA Cancer J Clin.

2004;54(3):131-49; quiz 82-4. doi: 10.3322/canjclin.54.3.131. PubMed PMID: 15195788.

12. Forkasiewicz A, Dorociak M, Stach K, Szelachowski P, Tabola R, Augoff K. The usefulness of lactate dehydrogenase measurements in current oncological practice. Cell Mol Biol Lett. 2020;25:35. Epub 20200609. doi: 10.1186/s11658-020-00228-7. PubMed PMID: 32528540; PubMed Central PMCID: PMCPMC7285607.

13. Tapia P, Soto D, Bruhn A, Alegria L, Jarufe N, Luengo C, et al. Impairment of exogenous lactate clearance in experimental hyperdynamic septic shock is not related to total liver hypoperfusion. Crit Care. 2015;19:188. Epub 20150422. doi: 10.1186/s13054-015-0928-3. PubMed PMID: 25898244; PubMed Central PMCID: PMCPMC4432956.

14. Hernandez G, Bellomo R, Bakker J. The ten pitfalls of lactate clearance in sepsis. Intensive Care Med. 2019;45(1):82-5. Epub 20180512. doi: 10.1007/s00134-018-5213-x. PubMed PMID: 29754310; PubMed Central PMCID: PMCPMC6334727.

15. Dmour HH, Khreisat EF, Khreisat AF, Hasan SA, Atoom O, Alkhatib AJ. Assessment of Lactate Dehydrogenase Levels Among Diabetic Patients Treated in the Outpatient Clinics at King Hussein Medical Center, Royal Medical Services, Jordan. Med Arch. 2020;74(5):384-6. doi: 10.5455/medarh.2020.74.384-386. PubMed PMID: 33424095; PubMed Central PMCID: PMCPMC7780787.

16. Hsieh YS, Yeh MC, Lin YY, Weng SF, Hsu CH, Huang CL, et al. Is the level of serum lactate dehydrogenase a potential biomarker for glucose monitoring with type 2 diabetes mellitus? Front Endocrinol (Lausanne). 2022;13:1099805. Epub 20221215. doi: 10.3389/fendo.2022.1099805. PubMed PMID: 36589820; PubMed Central PMCID: PMCPMC9801409.

17. Butt AA, Michaels S, Kissinger P. The association of serum lactate dehydrogenase level with selected opportunistic infections and HIV progression. Int J Infect Dis. 2002;6(3):178-81. doi: 10.1016/s1201-9712(02)90107-4. PubMed PMID: 12718831.

18. Wu MY, Yao L, Wang Y, Zhu XY, Wang XF, Tang PJ, et al. Clinical evaluation of potential usefulness of serum lactate dehydrogenase (LDH) in 2019 novel coronavirus (COVID-19) pneumonia. Respir Res. 2020;21(1):171. Epub 20200706. doi: 10.1186/s12931-020-01427-8. PubMed PMID: 32631317; PubMed Central PMCID: PMCPMC7336103.

19. Rechsteiner MC. Drosophila lactate dehydrogenase and alpha-glycerolphosphate dehydrogenase: distribution and change in activity during development. J Insect Physiol. 1970;16(6):1179-92. doi: 10.1016/0022-1910(70)90208-8. PubMed PMID: 5469747.

20. Tennessen JM, Baker KD, Lam G, Evans J, Thummel CS. The Drosophila estrogen-related receptor directs a metabolic switch that supports developmental growth. Cell Metab. 2011;13(2):139-48. doi: 10.1016/j.cmet.2011.01.005. PubMed PMID: 21284981; PubMed Central PMCID: PMCPMC3072597.

21. Robert B. Church FWR. A biochemical study of the growth of Drosophila

melanogaster. Journal of experimental Zoology. 1966. doi: https://doi.org/10.1002/jez.1401620309Citations.

22. Li H, Rai M, Buddika K, Sterrett MC, Luhur A, Mahmoudzadeh NH, et al. Lactate dehydrogenase and glycerol-3-phosphate dehydrogenase cooperatively regulate growth and carbohydrate metabolism during Drosophila melanogaster larval development. Development. 2019;146(17). Epub 20190912. doi: 10.1242/dev.175315. PubMed PMID: 31399469; PubMed Central PMCID: PMCPMC6765128.

23. Wong KKL, Verheyen EM. Metabolic reprogramming in cancer: mechanistic insights from Drosophila. Dis Model Mech. 2021;14(7):1-17. Epub 20210709. doi: 10.1242/dmm.048934. PubMed PMID: 34240146; PubMed Central PMCID: PMCPMC8277969.

24. Volkenhoff A, Weiler A, Letzel M, Stehling M, Klämbt C, Schirmeier S. Glial Glycolysis Is Essential for Neuronal Survival in Drosophila. Cell Metab. 2015;22(3):437-47. Epub 20150730. doi: 10.1016/j.cmet.2015.07.006. PubMed PMID: 26235423.

25. González-Gutiérrez A, Ibacache A, Esparza A, Barros LF, Sierralta J. Neuronal lactate levels depend on glia-derived lactate during high brain activity in Drosophila. Glia. 2020;68(6):1213-27. Epub 20191226. doi: 10.1002/glia.23772. PubMed PMID: 31876077.

26. Liu L, MacKenzie KR, Putluri N, Maletić-Savatić M, Bellen HJ. The Glia-Neuron Lactate Shuttle and Elevated ROS Promote Lipid Synthesis in Neurons and Lipid Droplet Accumulation in Glia via APOE/D. Cell Metab. 2017;26(5):719-37.e6. Epub 20170928. doi: 10.1016/j.cmet.2017.08.024. PubMed PMID: 28965825; PubMed Central PMCID: PMCPMC5677551.

27. Niccoli T, Kerr F, Snoeren I, Fabian D, Aleyakpo B, Ivanov D, et al. Activating transcription factor 4-dependent lactate dehydrogenase activation as a protective response to amyloid beta toxicity. Brain Commun. 2021;3(2):fcab053. Epub 20210326. doi: 10.1093/braincomms/fcab053. PubMed PMID: 33977265; PubMed Central PMCID: PMCPMC8093921.

28. Krejcova G, Danielova A, Nedbalova P, Kazek M, Strych L, Chawla G, et al. Drosophila macrophages switch to aerobic glycolysis to mount effective antibacterial defense. Elife. 2019;8. Epub 20191014. doi: 10.7554/eLife.50414. PubMed PMID: 31609200; PubMed Central PMCID: PMCPMC6867711.

29. Eichenlaub T, Villadsen R, Freitas FCP, Andrejeva D, Aldana BI, Nguyen HT, et al. Warburg Effect Metabolism Drives Neoplasia in a Drosophila Genetic Model of Epithelial Cancer. Curr Biol. 2018;28(20):3220-8 e6. Epub 20181004. doi: 10.1016/j.cub.2018.08.035. PubMed PMID: 30293715.

30. Wang CW, Purkayastha A, Jones KT, Thaker SK, Banerjee U. In vivo genetic dissection of tumor growth and the Warburg effect. Elife. 2016;5. Epub 20160901. doi: 10.7554/eLife.18126. PubMed PMID: 27585295; PubMed Central PMCID:

PMCPMC5030086.

31. Wong KKL, Liao JZ, Verheyen EM. A positive feedback loop between Myc and aerobic glycolysis sustains tumor growth in a Drosophila tumor model. Elife. 2019;8. Epub 20190701. doi: 10.7554/eLife.46315. PubMed PMID: 31259690; PubMed Central PMCID: PMCPMC6636907.

32. Bawa S, Brooks DS, Neville KE, Tipping M, Sagar MA, Kollhoff JA, et al. Drosophila TRIM32 cooperates with glycolytic enzymes to promote cell growth. Elife. 2020;9. Epub 20200330. doi: 10.7554/eLife.52358. PubMed PMID: 32223900; PubMed Central PMCID: PMCPMC7105379.

33. Feng T, Zhao X, Gu P, Yang W, Wang C, Guo Q, et al. Adipocyte-derived lactate is a signalling metabolite that potentiates adipose macrophage inflammation via targeting PHD2. Nat Commun. 2022;13(1):5208. Epub 20220905. doi: 10.1038/s41467-022-32871-3. PubMed PMID: 36064857; PubMed Central PMCID: PMCPMC9445001.

34. Abu-Shumays RL, Fristrom JW. IMP-L3, A 20-hydroxyecdysone-responsive gene encodes Drosophila lactate dehydrogenase: structural characterization and developmental studies. Dev Genet. 1997;20(1):11-22. doi: 10.1002/(SICI)1520-6408(1997)20:1<11::AID-DVG2>3.0.CO;2-C. PubMed PMID: 9094207.

35. Lavista-Llanos S, Centanin L, Irisarri M, Russo DM, Gleadle JM, Bocca SN, et al. Control of the hypoxic response in Drosophila melanogaster by the basic helix-loop-helix PAS protein similar. Mol Cell Biol. 2002;22(19):6842-53. doi: 10.1128/MCB.22.19.6842-6853.2002. PubMed PMID: 12215541; PubMed Central PMCID: PMCPMC134029.

36. Quinones-Coello AT, Petrella LN, Ayers K, Melillo A, Mazzalupo S, Hudson AM, et al. Exploring strategies for protein trapping in Drosophila. Genetics. 2007;175(3):1089-104. Epub 20061218. doi: 10.1534/genetics.106.065995. PubMed PMID: 17179094; PubMed Central PMCID: PMCPMC1840052.

37. Li H, Tennessen JM. Methods for studying the metabolic basis of Drosophila development. Wiley Interdiscip Rev Dev Biol. 2017;6(5). Epub 20170526. doi: 10.1002/wdev.280. PubMed PMID: 28556549; PubMed Central PMCID: PMCPMC5561480.

38. Li H, Chawla G, Hurlburt AJ, Sterrett MC, Zaslaver O, Cox J, et al. Drosophila larvae synthesize the putative oncometabolite L-2-hydroxyglutarate during normal developmental growth. Proc Natl Acad Sci U S A. 2017;114(6):1353-8. Epub 20170123. doi: 10.1073/pnas.1614102114. PubMed PMID: 28115720; PubMed Central PMCID: PMCPMC5307464.

39. Cox JE, Thummel CS, Tennessen JM. Metabolomic Studies in Drosophila. Genetics. 2017;206(3):1169-85. doi: 10.1534/genetics.117.200014. PubMed PMID: 28684601; PubMed Central PMCID: PMCPMC5500124.

40. Li H, Tennessen JM. Preparation of Drosophila Larval Samples for Gas

Chromatography-Mass Spectrometry (GC-MS)-based Metabolomics. J Vis Exp. 2018;(136). Epub 20180606. doi: 10.3791/57847. PubMed PMID: 29939167; PubMed Central PMCID: PMCPMC6101626.

41. Nolo R, Abbott LA, Bellen HJ. Senseless, a Zn finger transcription factor, is necessary and sufficient for sensory organ development in Drosophila. Cell. 2000;102(3):349-62. doi: 10.1016/s0092-8674(00)00040-4. PubMed PMID: 10975525.

42. Huang F, Dambly-Chaudiere C, Ghysen A. The emergence of sense organs in the wing disc of Drosophila. Development. 1991;111(4):1087-95. doi: 10.1242/dev.111.4.1087. PubMed PMID: 1879352.

43. Brown JB, Boley N, Eisman R, May GE, Stoiber MH, Duff MO, et al. Diversity and dynamics of the Drosophila transcriptome. Nature. 2014;512(7515):393-9. doi: 10.1038/nature12962. PubMed PMID: 24670639; PubMed Central PMCID: PMCPMC4152413.

44. Mahmoudzadeh NH, Fitt AJ, Schwab DB, Martenis WE, Nease LM, Owings CG, et al. The oncometabolite L-2-hydroxyglutarate is a common product of dipteran larval development. Insect Biochem Mol Biol. 2020;127:103493. Epub 20201103. doi: 10.1016/j.ibmb.2020.103493. PubMed PMID: 33157229; PubMed Central PMCID: PMCPMC7704715.

45. Callier V, Hand SC, Campbell JB, Biddulph T, Harrison JF. Developmental changes in hypoxic exposure and responses to anoxia in Drosophila melanogaster. J Exp Biol. 2015;218(Pt 18):2927-34. Epub 20150723. doi: 10.1242/jeb.125849. PubMed PMID: 26206351.

46. Liu L, MacKenzie KR, Putluri N, Maletic-Savatic M, Bellen HJ. The Glia-Neuron Lactate Shuttle and Elevated ROS Promote Lipid Synthesis in Neurons and Lipid Droplet Accumulation in Glia via APOE/D. Cell Metab. 2017;26(5):719-37 e6. Epub 20170928. doi: 10.1016/j.cmet.2017.08.024. PubMed PMID: 28965825; PubMed Central PMCID: PMCPMC5677551.

47. Natzle JE, Hammonds AS, Fristrom JW. Isolation of genes active during hormone-induced morphogenesis in Drosophila imaginal discs. J Biol Chem. 1986;261(12):5575-83. PubMed PMID: 3007512.

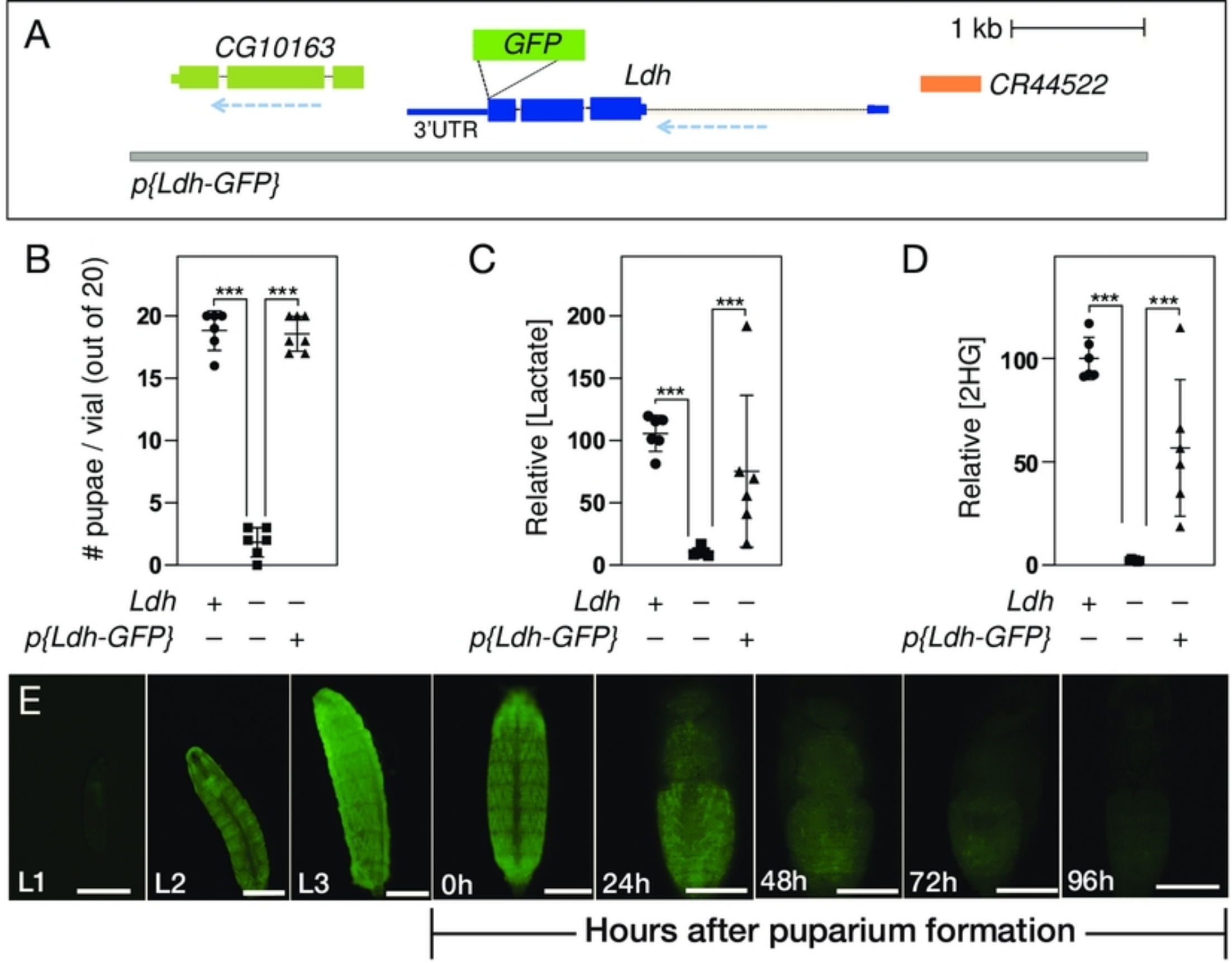

Figure 1. Genetic characterization of the *p{Ldh-GFP}* transgene. (A) A schematic diagram of the *Ldh-GFP*^{Genomic} transgene illustrating the placement of GFP immediately before the *Ldh* stop codon. When this transgene is placed in a *Ldh*$^{16/17}$ mutant background, the resulting Ldh-GFP fusion protein is capable of not only rescuing (B) the *Ldh* mutant lethal phenotype, but also restoring steady state levels of (C) lactate and (D) 2-hydroxyglutarate (2HG). (E) The *Ldh-GFP*^{Genomic} temporal expression pattern is consistent with previous studies, with Ldh-GFP^{Genomic} being expressed at high levels throughout larval development and then declining at the onset of metamorphosis. Data in (B-D) analyzed using one-way ANOVA followed by a post hoc Tukey HSD. ***P<0.001.

Figure 1

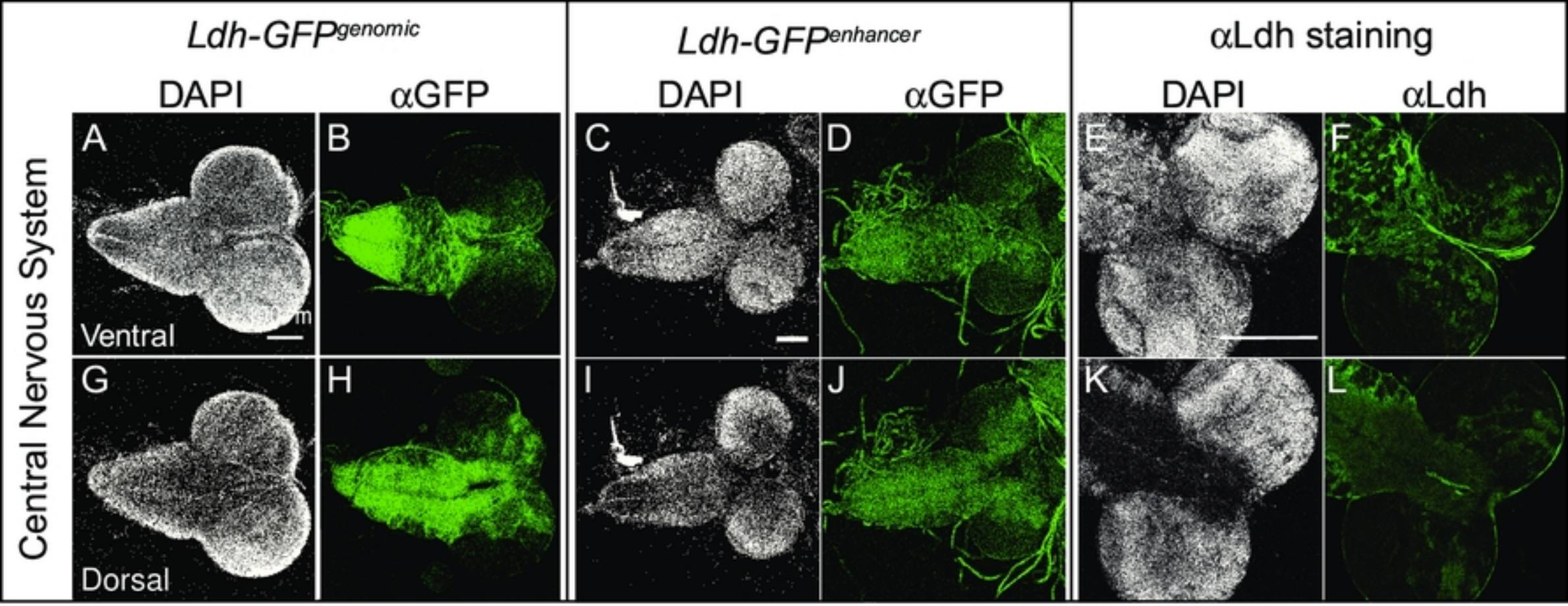

Figure 2. Characterization of *Ldh* expression in the central nervous system. The *Ldh* expression pattern in the central nervous system of L3 larvae was examined using *Ldh-GFP*^{Genomic}, *Ldh-GFP*^{enhancer}, and an αLdh antibody. (A-L) Representative confocal images of Ldh expression and DAPI staining in the (A-F) ventral and (G-L) dorsal sides of the CNS. For *Ldh-GFP*^{Genomic} and *Ldh-GFP*^{enhancer} expression analysis, the CNS was fixed and stained with an αGFP antibody as described in the methods. The scale bar in all images represents 40 μM. Scale bar in (A) applies to (B,G,H). Scale bar in (C) applies to (D,I,J). Scale bar in (E) applies to (F,K,L).

Figure 2

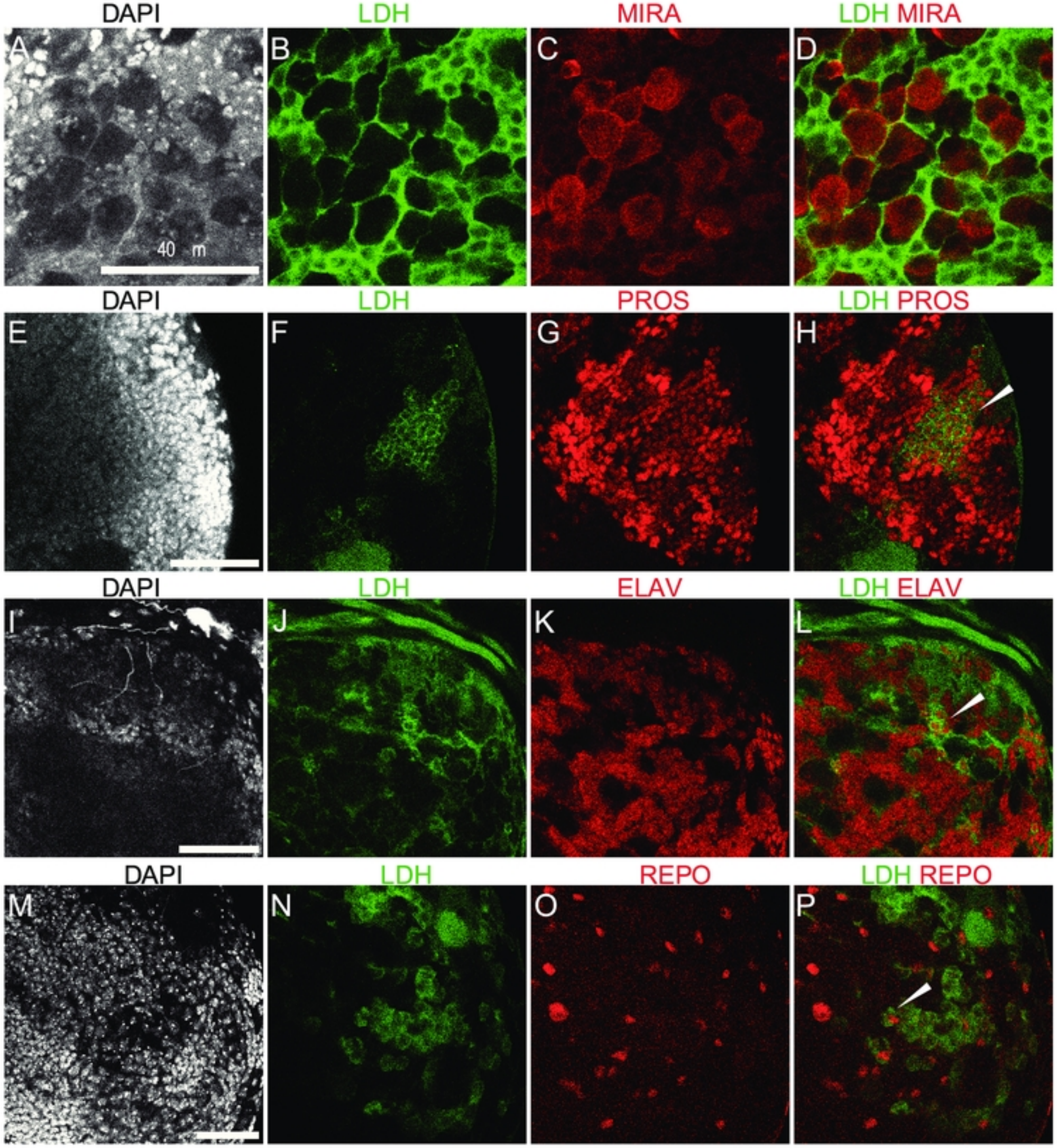

Figure 3. *Ldh* expression in ganglion mother cells, neurons, and glia. Representative confocal images showing the absence of *Ldh* in neuroblasts of third instar *Ldh-GFP* ^{genomic} larvae. The first two columns from left to right show DAPI and LDH. The last column shows the colocalization of *Ldh* with CNS cell specific markers. (A-D) *Ldh* is not expressed in neuroblasts, which are labelled with αMiranda (MIRA) antibody. In contrast, (E-H) *Ldh* is expressed in ganglion mother cells (GMCs), which are labelled with αProspero (PROS) antibody. Ldh-GFP is also present in both (I-K) neurons stained with αElav and (M-P) and glia stained with αRepo. For *Ldh-GFP*^{Genomic} and *Ldh-GFP*^{enhancer} expression analysis, the CNS was fixed and stained with an αGFP antibody as described in the methods. The scale bar in all images represents 40 μM. Scale bar in (A) applies to B-D). Scale bar in (E) applies to (F-H). Scale bar in (I) applies to (J-L). Scale bar in (M) applies to (N-P).

Figure 3

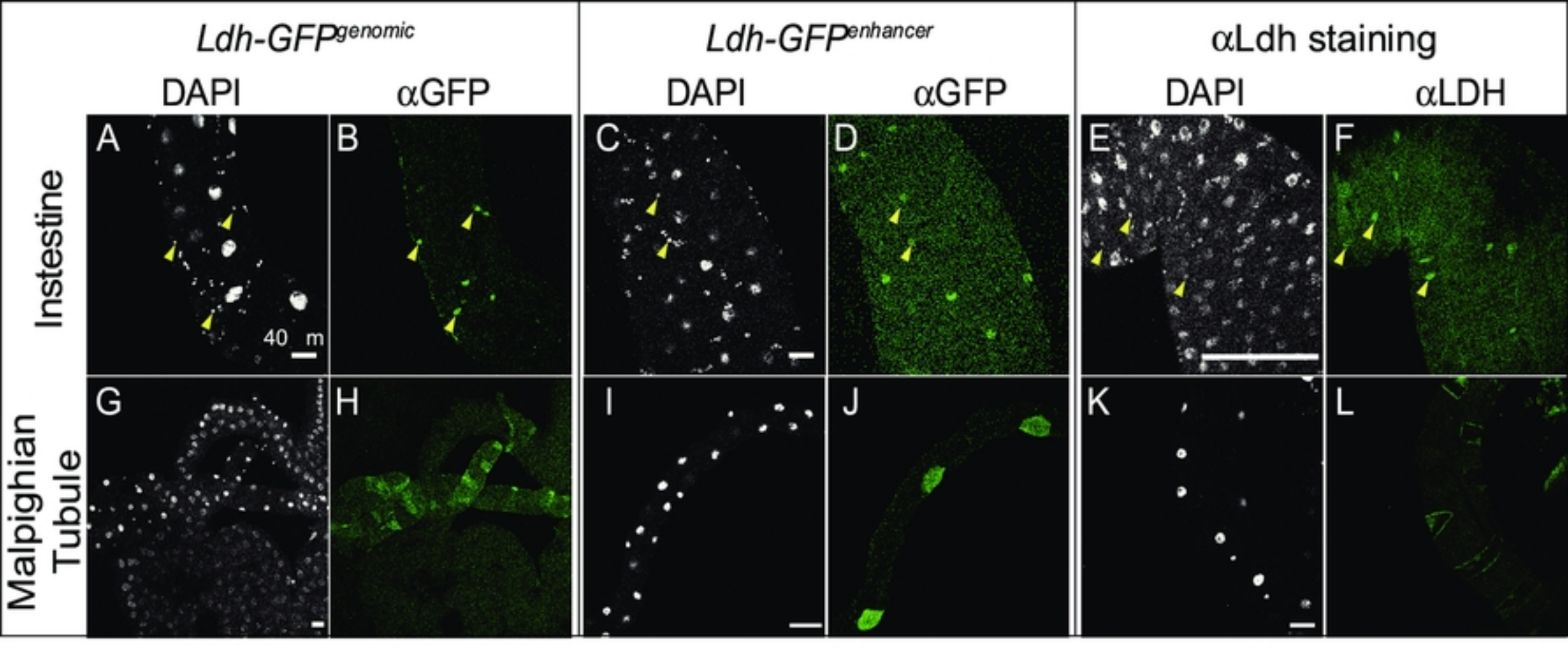

Figure 4. Characterization of *Ldh* expression in the intestine and Malpighian tubules. The *Ldh* expression pattern in the intestine and Malphigian tubules of L3 larvae was examined using *Ldh-GFP*^{Genomic}, *Ldh-GFP*^{enhancer}, and an αLdh antibody. (A-L) Representative confocal images of *Ldh* expression and DAPI staining in (A-F) the midgut and (G-L) the Malphigian tubules. Note that *Ldh* is expressed at significantly higher levels in (A,C,E) a subset of small cells of the AMP clusters (denoted with arrowheads in (A-F)) and (G,I,K) the stellate cells of the Malpighian tubules. For *Ldh-GFP*^{Genomic} and *Ldh-GFP*^{enhancer} expression analysis, tissues were fixed and stained with an αGFP antibody as described in the methods. The scale bar in all images represents 40 μM.

Figure 4

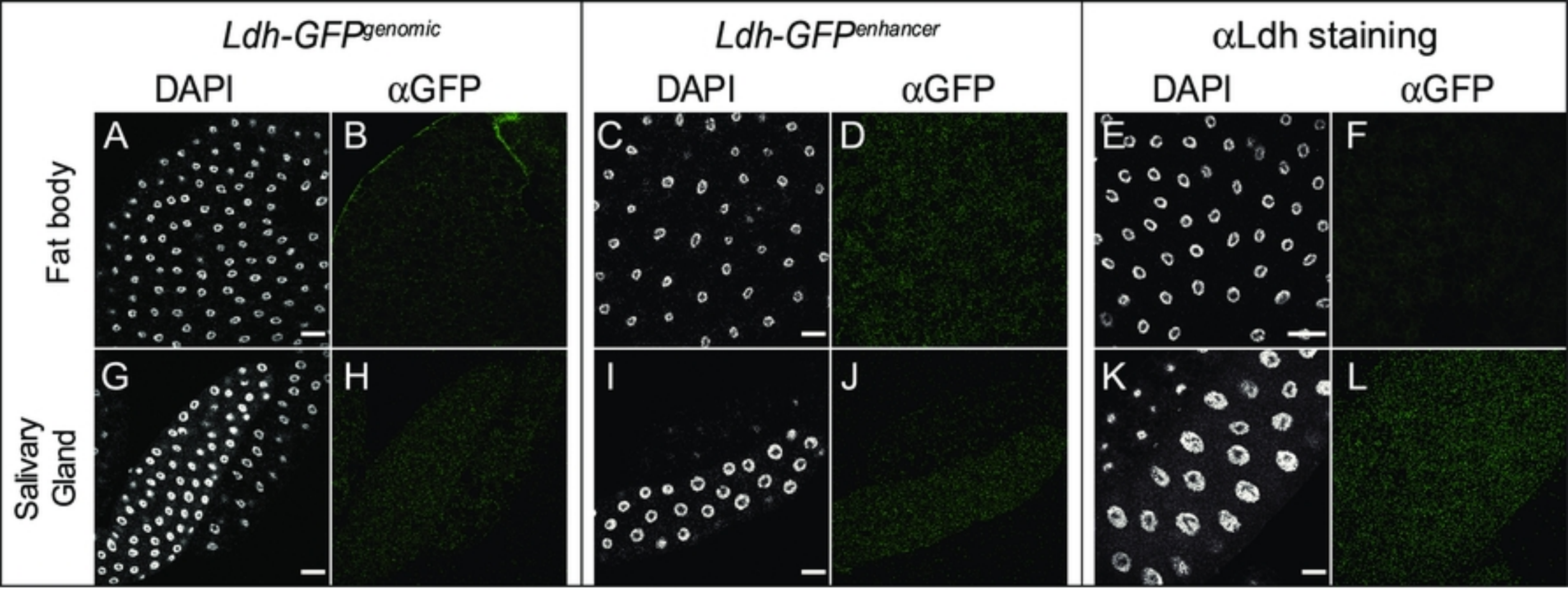

Figure 5. *Ldh* expression pattern in the fat body and salivary gland. The *Ldh* expression patterns in the fat body and salivary glands of L3 larvae were examined using *Ldh-GFP*^{Genomic} and *Ldh-GFP*^{enhancer}. (A-L) Representative confocal images of *Ldh* expression and DAPI staining in (A-F) the fat body and (G-L) the salivary glands. For *Ldh-GFP*^{Genomic} and *Ldh-GFP*^{enhancer} expression analysis, tissues were fixed and stained with an αGFP antibody as described in the methods. The scale bar in all images represents 40 μM.

Figure 5

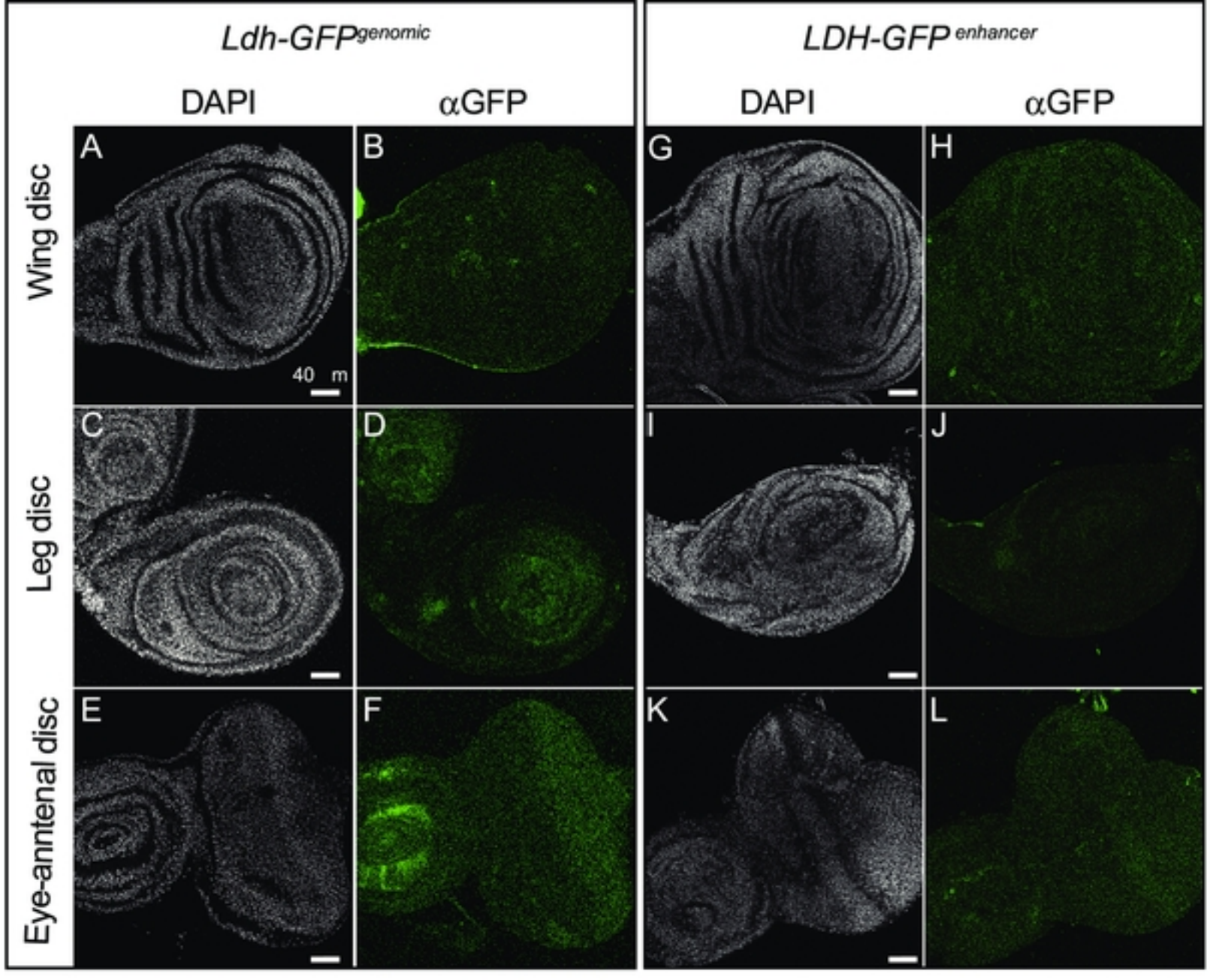

Figure 6. *Ldh* expression pattern in Imaginal discs. Representative confocal images of imaginal discs (top to bottom: wing disc, leg disc and eye disc) dissected from third instar (D5 AEL) *Ldh-GFP* ^{genomic} (A-F) and *Ldh-GFP*^{enhancer} (G-L) third instar larvae. DAPI is shown in white and *Ldh* expression is shown in green. Note that the αLdh antibody failed to produce any staining in the imaginal discs and thus were excluded from the figure. The scale bar in all images represents 40 μM.

Figure 6